Development of a FBG Based Hoop-Strain Sensor Using 3D Printing Method

CHENGYU HONG[ID][1]**, YIFAN ZHANG**[2]**, DONG SU**[1]**, AND ZHENYU YIN**[3]

[1]College of Civil and Transportation Engineering, Shenzhen University, Shenzhen 518060, China
[2]Shenzhen Zhongdi Construction Engineering Limited Company, Shenzhen 518060, China
[3]Department of Civil and Environmental Engineering, The Hong Kong Polytechnic University, Hong Kong

Corresponding author: Yifan Zhang (tcyifan@126.com)

ABSTRACT In this study, a hoop-strain sensor was developed by embedding a bare fiber Bragg grating (FBG) sensor inside 3D printed Polylactic Acid (PLA) filament. Fabrication process of the hoop-strain sensor indicates that the initial temperature of the melted PLA is around 50 °C which is obviously lower than the printing temperature of the printer nozzle (around 200°C). A typical residual wavelength was found after the fabrication process of the hoop-strain sensor. The shrinkage deformation of the present sensor was around 208 $\mu\varepsilon$ after fabrication. The hoop-strain sensor was flexible and can be used to measure both circumferential strain change and contact pressure between hoop-strain sensors and cylinders. Calibration tests for elongation measurement indicate that the sensitivity and minimum resolution with respect to strain change are 4.04 nm/% and 3.574 $\mu\varepsilon$, respectively. The obtained measurement sensitivity and resolution for pressure measurement were 0.0035 nm/kPa, and 0.286 kPa, respectively. The maximum measurement ranges of the hoop-strain sensor for strain and pressure measurement are larger than 1% and 800 kPa, respectively.

INDEX TERMS Hoop-strain sensor, fiber Bragg grating, 3D printing, polylactic acid, circumferential strain.

I. INTRODUCTION

Fiber Bragg grating (FBG) has been a reliable, in situ, non-destructive sensing technique for health monitoring and diagnostics of civil infrastructures. FBG sensors have been widely used due to a number of outstanding advantages such as versatility to measure different parameters, insensitivity to electromagnetic fields and corrosion, multiplexing capability, small size, and high sensitivity [1], [2]. Bare FBG sensors have been widely used for the design and fabrication of a large variety of sensors which were applied for the field monitoring under harsh monitoring environment such as highly corrosion, high temperature, and high humidity.

Hoop-strain sensor is a nondestructive method to measure circumferential strain of cylinders or pipes for the detection of integrity, leakage and corrosion [3]. Optical fiber sensors such as FBG sensors [4], Brillion optical time domain analysis (BOTDA), and Brillion optical time domain reflectometry (BOTDR) are mostly used for the fabrication of different hoop-strain sensors due to their advantages of real-time monitoring, high resolution and long-term reliability [5], [6]. FBG sensor is a suitable sensing technology to fabricate different types of hoop-strain sensors. For example, FBG sensor can be fabricated into two gripper tubes with a movable end and a fixed end to form a hoop-strain sensor, which was used to monitor the circumferential strain change of PVC model pipelines [7]–[9]. FBG based hoop-strain sensor can also be developed and mounted in the axial directions of a FRP pressure vessel to monitor the strain status during its pressurization [10]. Corrosion of steel bars can also be monitored in real-time by surrounding with FBGs. These hoop-strain sensors were found ease of use and can successfully predict the safety status of measured objects. However, most of the adopted sensors were found relatively complicated in fabrication procedures (such as assembling different hoop-strain sensor components), and installation process (such as surrounding steel bars with FBGs).

3D printing technique is a quick method for the fabrication of functional objects. The combination of 3D printing method and other sensing technologies can be used to create various sensors [11]–[15]. Due to the advantages of small size and high flexibility, bare FBG sensors can be well integrated into
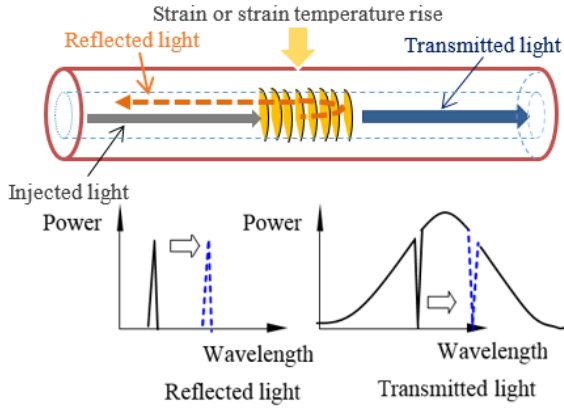
FIGURE 1. Work principle of fiber Bragg grating sensor.

FIGURE 2. Sensing diagram of the FBG hoop-strain sensor.

3D printed prototypes to form various new sensors such as tilt sensors [16], flexion sensors [17], pressure sensors [18], goniometers [19], and displacement sensors [1]. Past investigations proved that FBG sensors can be successfully embedded inside 3D printed prototypes [20]. A new FBG pressure transducer was developed by embedding a bare FBG inside 3D printed acrylonitrile butadiene styrene (ABS) filament to measure hydrostatic pressure [21]. But the design of internal sensor components appears to be complicated, so that it may be difficult to realize the encapsulation process for FBG sensors. Some investigations also concern using FBG sensors and 3D printing method to fabricate more durable strain sensors [22], but the FBGs were mounted at the surface using glue rather than embedding inside 3D printed prototypes. The FBGs can be fully coupled with printed materials if embedded during printing process rather than fixed on surface of sensor components. Even there are some studies have been found using 3D printing and FBG sensors to design new strain sensors [23], few studies have been reported focusing on the applications of 3D printing method to fabricate hoop-strain sensors based on FBG sensors.

In this study, we fabricate a 3D printed FBG hoop-strain sensor which can be used to measure both elongation and contact pressure. Objectives of this study are (a) development of a simple and ease of use hoop-strain sensor based on FBG sensing technology and 3D printing method; (b) verification of the fabrication process of FBG hoop-strain sensor and examination of FBG signal change during melting and hardening process of PLA filament; and (c) performance testing and validation of FBG hoop-strain sensors for the measurement of deformation and pressure.

II. DESIGN AND OF A FBG HOOP-STRAIN SENSOR
A. SENSING PRINCIPLE OF FBG SENSOR
Working principle of FBGs is mainly based on the principle of Bragg reflection. Fig.1 shows a schematic view of sensing principle of a FBG sensor. When broadband light is injected into fiber core, passing through the grating position, where the light will be in phase, amplified and reflected. Bragg
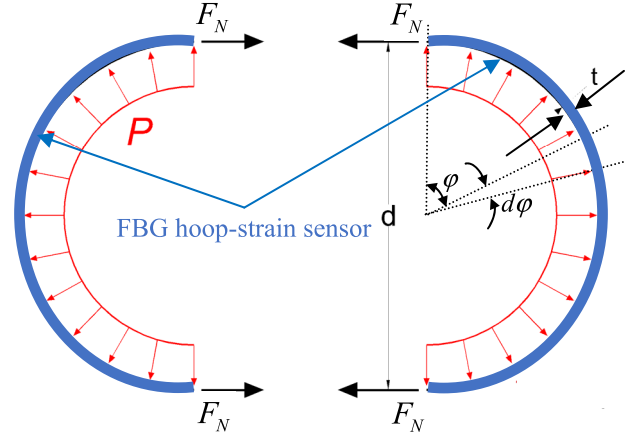
wavelength variation can be expressed as:

$$\frac{\Delta\lambda}{\lambda} = (1 - p_{eff})\Delta\varepsilon + (\alpha + \xi)\Delta T \tag{1}$$

where $\Delta\lambda$, and λ are wavelength change and initial wavelength of FBG, respectively. $\Delta\varepsilon$ and ΔT are longitudinal strain and temperature change, respectively. p_{eff}, α and ξ are photo-elastic constant, thermal expansion coefficient and thermal-optic coefficient, respectively.

B. DESIGN OF A FBG BASED HOOP-STRAIN SENSOR
A simple flexible FBG based hoop-strain sensor is designed and fabricated by directly embedding a bare FBG sensor into 3D printed PLA ring. Figure 2 presents a diagram of sensing mechanism of the hoop-strain sensor mounted on a cylinder with internal pressure (or uniform contact pressure between hoop-strain sensor and the mounted cylinder). The internal contact pressure between cylinder and hoop-strain sensor induces a resultant tension force F_N along the axis of hoop-strain sensor, as shown in Figure 2. The resultant force F_R along the direction of F_N can be determined by integration of internal pressure P as follows:

$$F_R = \int_0^\pi (Pl\frac{d}{2}d\varphi)\sin\varphi = Pld \tag{2}$$

where l and d are length and diameter of the cross section, respectively. The resultant tension force can be given by:

$$F_N = \frac{1}{2}F_R = \frac{1}{2}Pld \tag{3}$$

Thickness and width of the FBG hoop-strain sensor are t and w respectively, as shown in Figure 2. Tension strain of the hoop-strain sensor can therefore be determined by:

$$\Delta\varepsilon = \frac{\Delta F_N}{EA} = \frac{\Delta Pld}{2Ewt} \tag{4}$$

The final correlation between wavelength change ratio and contact pressure change can be obtained by combing Eq. (1) and Eq.(4) as follows:

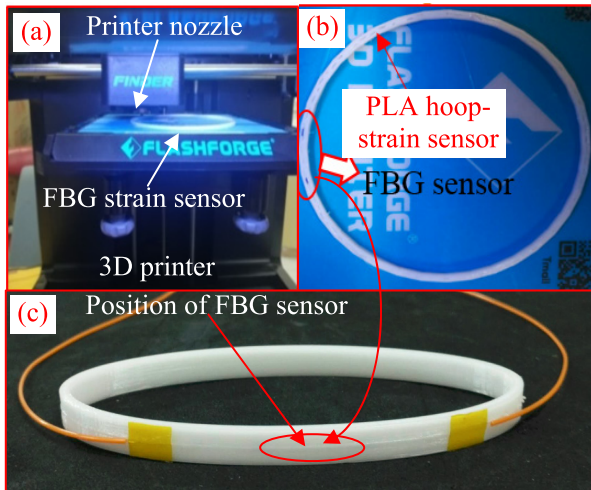$$\frac{\Delta\lambda}{\lambda} = \Delta P \frac{ld(1 - p_{eff})}{2Ewt} \tag{5}$$

FIGURE 3. A FBG hoop-strain sensor fabricated using 3D printing method.

FIGURE 4. Variation of FBG wavelength change before, during and after printing process.

Therefore, the wavelength change ratio can be used not only to compute the elongation of cylinder perimeter but also to calculate the contact pressure between FBG hoop-strain sensor and the measured cylinder. In this study, a bare FBG will be embedded inside the sensing section of the hoop-strain sensor to measure the occurred tension strain, as marked by blue color in Figure 2.

C. SENSOR FABRICATION AND VERIFICATION OF EMBEDDING A BARE FBG INSIDE PLA FILAMENT

This hoop-strain sensor is made of Polylactic Acid (PLA) material, which is flexible in nature. Design and fabrication process of the FBG based hoop-strain sensor is presented in Figure 3. A white color, big size PLA ring is created inside the 3D printer as shown in Figure 3a. Dimension of this PLA ring are 80 mm × 85 mm × 5 mm (inner diameter × external diameter × thickness). The nozzle inside the 3D printer extruded the PLA filament layer by layer, forming a round ring where a bare FBG is embedded inside when 50% size of the ring is completed (Figure 3b). The bare FBG was placed on the upper surface of the cross section of PLA ring, and fixed using tapes at the two ends of the FBG section. Then the 3D printer continues to print the rest part of the PLA ring. The final completed FBG-hoop strain sensor is shown in Figure 3c.

This fabricated PLA ring is finished within 10 minutes inside the 3D printer. Encapsulation of FBG inside PLA takes around 30 seconds during printing process. Fabrication of different 3D models using different filaments such as acrylonitrile butadiene styrene copolymers (ABS), polylactic acid (PLA), polyvinyl chloride (PVC), and thermoplastic polyurethanes (TPU) normally involves heating the above raw filament materials into liquid. Printing temperature of the printer nozzle exceeds 200 °C, which may damage the measurement performance of FBG. To verify the feasibility of embedding FBG inside printed prototypes, the FBG wavelength change was continuously collected from the embedded FBG during printing process. Figure 4 presents FBG
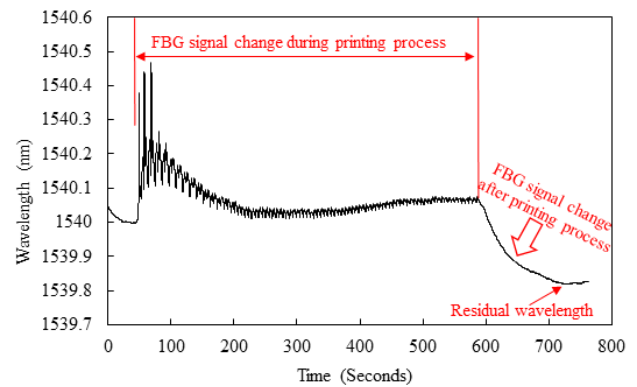
wavelength variation against time during printing process inside the 3D printer. It is clear that the wavelength change during printing process is characterized by a significant initial wavelength fluctuation (during 80-200 seconds as shown in Figure 3). This phenomenon is mainly due to the interaction between melted PLA and FBG, leading to a maximum wavelength rise of around 0.5 nm (around 50°C rise in temperature). Then the FBG wavelength becomes relatively stable after 200 seconds as printing continuous, approaching around 1540.05 nm at 600 seconds before finishing the whole prototype inside 3D printer. The collected wavelength values of FBG exhibit a sudden drop at around 720 seconds with a residual wavelength 1539.8 nm being obtained. The occurred residual wavelength is mainly a result of the hardening process of PLA material, leading to both deformation shrinkage and temperature decrease of PLA prototype. The decrease in temperature (after 600 seconds) from melting point to room temperature induces a strain reduction 208 $\mu\varepsilon$ (from 1540.05 nm to 1539.8 nm) of the PLA filament. The embedded bare FBG sensor successfully measured strain change of the PLA prototype during the whole printing process even the printing temperature of the nozzle exceeds 220°C.

III. PERFORMANCE EVALUATION OF FBG HOOP-STRAIN SENSORS

Measurment performance of the new FBG hoop-strain sensor was examined using two series of calibratoin tests, including (a) direct elongation measurment under different tension strain, and (b) circumferential strain measurement of a PE cynlinder.

A. ELONGATION MEASUREMENT

Elongation measurement was condcuted in laboratory by directly applying tension displacement on the hoop-strain sensor. Figure 5 shows a schematic side view of calibration setup. The hoop-strain sensor was mounted on a calibration platform which is very stable in lab. FBG sensor was at the center and the two ends were fixed on micro-displacement platform. A linear variable displacement transducer was used to measure and control the tension displacement. The tension strain was applied step by step with a strain increment of
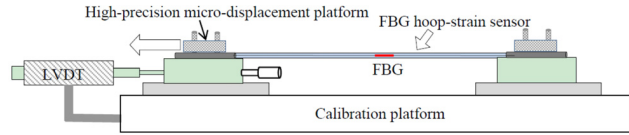
FIGURE 5. A schematic view of calibration setup of the hoop-strain sensor.
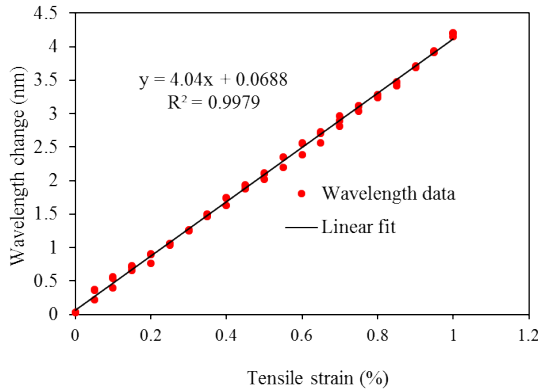

FIGURE 6. Relationship between wavelength change and tensile strain in calibration test.

0.05% and a maximum tension strain of 1% was finally approached. FBG wavelength data were continuously collected by interrogator at a frequency of 10 Hz. Figure 5 shows the wavelegnth change of FBG hoop-strain sensor agaisnt applied tension strain. It is clear that a straight linear line can be used to fit the relationship between wavelength change and tension strain. Standard deviation and mean value of measurement errors (with respect to the fitted linear wavelength data) in the elogation tests are −0.022 and 0.0408 nm, respectively. The maximum and minimum errors of measured wavelength values are 0.0657 and −0.1163 nm, respectively. The final sensitivity and resolution of the FBG hoop-strain sensor for circumferential strain measurement are 4.04 nm/% and 2.475 $\mu\varepsilon$, respectively.

Three cyclic elongation tests were conducted on the hoop-strain sensor. The applied strain for three elongation cycles were 0.1%, 0.2%, and 0.3%, respectively. Elongation rates of the hoop-strain sensor were 0.1%/100s, 0.2%/100s, and 0.3%/100s, respectively. Figures 7a, b and c present the relationships of wavelength change against time in three cyclic elongation tests. A total of 7 peak wavelength values can be observed in each figure. The obtained cyclic change in wavelength values are highly consistent in the three figures. The larger the elongation deformation, the larger the wavelength difference. The occurred recoverable wavelength variations indicate that the FBG hoop-strain sensor is still within elasticity range. It is noted that there is a stable phase after each loading cycle in Figure 7a, and this is because we specified a special loading interval (around 40 seconds) for each loading cycle in the first elongation test. After we verified the measurement performance, we removed this loading interval and obtained the measured wavelength change continuously
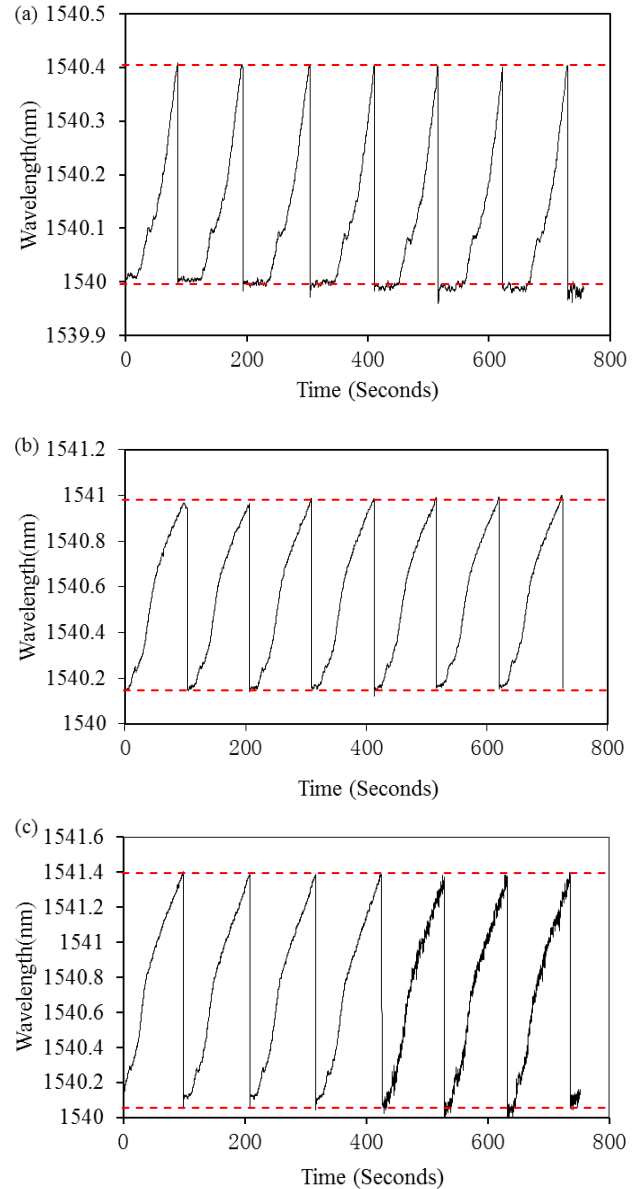

FIGURE 7. Measured wavelength change against time at different cyclic elongation tests with tension strains of (a) 0.1%, (b) 0.2%, and (c) 0.3%.

in Figures 7b and c. In addition, the minimum wavelength values are slightly different, this may be due to the unstable laboratory temperature which would result in certain wavelength shift of FBG sensors.

Wavelength ratio $\Delta\lambda/\lambda$ as shown in Eq.(1) directly reflects the occurred strain change. Figure 8 shows relationships of wavelength ratios against number of cycles in elongation tests at the tension strains of 0.1%, 0.2%, and 0.3%, respectively. The measured wavelength ratios of the three different tension strains are consistent. The larger the tension strain, the higher the wavelength ratio. The wavelength ratio also appears to increase linearly as the rise of tension strain. The maximum measurement error of all three tests is less than 9.6%.
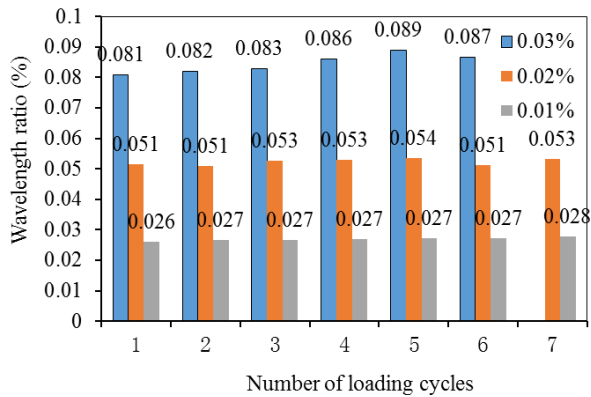
FIGURE 8. Relationships of wavelength ratio against number of cycles in cyclic elongation tests.
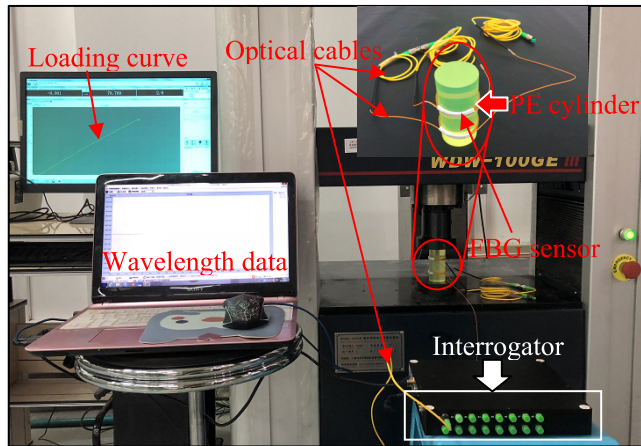

FIGURE 9. Experiment setup of cyclic loading test on a PE cylinder.

B. CIRCUMFERENTIAL STRAIN MEASUREMENT OF A PE CYLINDER

A cyclic loading test was also carried out on a polyethylene (PE) cylinder, which was mounted with two FBG hoop-strain sensors as shown in Figure 9. The color of the sensor belt mounted on the PE cylinder was yellow, and a thin white tape was used to protect the two ends of internal FBG sensor, in order to avoid optical fiber (two ends of FBG) detach from PLA when large deformation occurs.The PE cylinder was 40 mm in diameter and 80 mm in height before testing.The hoop-strain sensor is 40 mm in inner diameter and veryflexible, and hence can be tightly mounted on the PEcylinder. The circumferential strain of the PE cylinder can be monitored by the hoop-strain sensors as the lateral expansion will lead to tension deformation of the hoop-strain sensors. The PE cylinder was 40 mm in diameter and 80 mm in height before testing. Vertical pressure was applied step by step with a load increment of 40 kPa in each step, and the maximum vertical pressure on the top surface of PE cylinder was 800 kPa. Wavelength data of FBG hoop-strain sensors were continuously collected by optical interrogator at a frquency of 10 Hz.

Relationship between wavelength change and vertical pressure is shown in Figure 10. The occurred wavelength change at different vertical pressures can be fitted by a linear line. Sensitivity of wavelength change against vertical
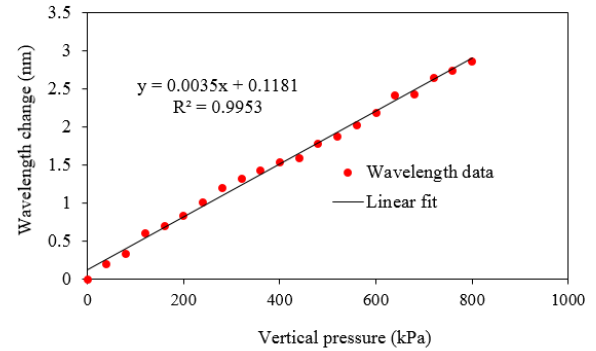

FIGURE 10. Measured relationship of wavelength change against applied vertical pressure.

pressure of the current FBG hoop-strain sensor is 0.0035 nm/kPa. As the minimum resolution of the present interrogator is 0.001 nm, so that the minimum resolution of FBG hoop-strain sensor for pressure measurement is 0.001 nm /0.0035 nm/kPa = 0.286 kPa. The maximum vertical pressure is 800 kPa, indicating that the measurement range of the present FBG hoop-strain sensor can be larger than 0-800 kPa.

Figure 11 illustrates cyclic change of FBG wavelength agasint time for the FBG hoop-strain sensor mounted at the the PE cylinder under different vertical pressures. Vertical pressures (including 150 kPa, 300 kPa, and 450 kPa) were applied on the top surface of the PE cynlinder, leading to a related wavelength difference of around 0.32 nm, 0.67 nm, and 0.99 nm, respectively. The obtained wavelenght difference varied almost linearly against the magnitudes of applied vertical pressure. Hence the wavelength change of FBG hoop-strain sensor can also be used to monitor the vertical pressure change of PE cylinders. Figure 11 presents the calcualted wavelength ratios of FBG hoop-strain sensor at 10 loading cycles. The maximum measurement errors with repsect to the average wavelength ratio at loading levels of 150 kPa, 300 kPa, and 450 kPa are 7.1%, 5.1%, and 5.6%, respectively.

IV. DISSCUSSION

Many filaments are avialble for 3D printing with different mechanical properties, such as polylactic acid (PLA), acrylonitrile butadiene styrene copolymers (ABS), polyvinyl alcohol (PVA), Carbon fiber, polyvinyl chloride (PVC), Nylon, polycarbonate, thermoplastic polyurethanes (TPU), etc. The reason of selecting PLA filament in present study includes ease of printing, low printing temperature (180-230°C), high flexibility, and high strength combined with low shrinkage and low warping. But the durability of PLA is relatively low compare with most of other filaments. ABS is another alternative for printing various sensing components. ABS is characterized by the advantages of high durability, impact, and resistance with a medium strength. But ABS is relatively low in density (around 1000 kg/m^3) and harmful during printing process. In addition, ABS filament tends to warp if printed without a heated bed.
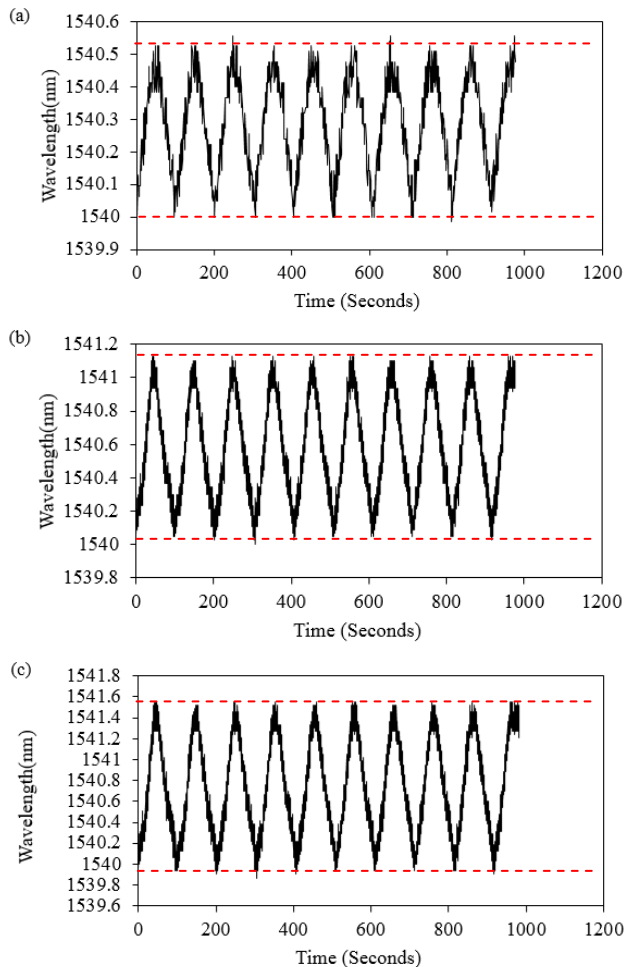
FIGURE 11. Cyclic cahnge of wavelneth agaisnt time in different cyclic loading tests when the vertical pressures were (a) 150 kPa, (b) 300 kPa, and (c) 450 kPa.
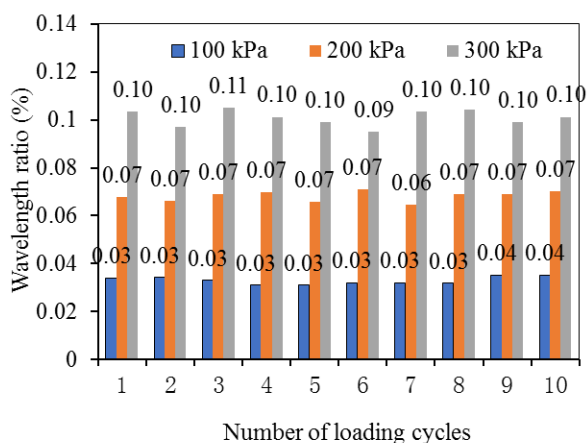

FIGURE 12. Relationships of wavelength ratio agianst number of loading cycles in (a) tension tests, and (b) uniaxial compression test.

PVA is also one non harmful, non-toxic filament (similar to PLA) for 3D printing. Advantages of PVA include environment friendly and easily stripping. The PVA filament can work well with PLA and nylon filaments as they require almost the same operating conditions. One main drawback of PVA is a hydrophilic material, so that the PVA material can easily connect with water molecules, leading to PVA dissolving in water. Hence the PVA may not be suitable for fabricating sensors which will be applied in relatively harsh environment underwater or with high humidity. Carbon fiber as a printing filament provides impressive rigidity, structure, layer adhesion and requires similar operating condition as PLA. Advantages of carbon fiber include ease of printing, high durability, little shrinkage and wrapping during printing and cooling process. In addition, carbon fiber is stiffer than PLA filament with better dimensional stability, and outstanding layer adhesion. Hence the sensor components fabricated using carbon fiber filament can be applied for relatively harsh measurement environment.

V. CONCLUSIONS

In this study, a bare FBG was embedded into 3D printed PLA filament to fabricate a hoop-strain sensor, which was successfully used to measure elongation and vertical pressure of a PE cylinder in uniaxial test. Typical findings and conclusions are drawn as follows:

(a) A hoop-strain sensor was developed using 3D printing method. The fabrication process of the hoop-strain sensor can be finished within 20 minutes. No glue or epoxy resin was used to fix FBG sensing section during encapsulation process of the hoop-strain sensors.

(b) Bare FBG sensors were successfully embedded into printed PLA filament during fabrication process inside a 3D printer. The fabrication process of PLA based hoop-strain sensor leads to a maximum temperature rise of around 50 °C. A final wavelength reduction of around 0.2 nm (corresponding to 208 $\mu\varepsilon$ shrinkage deformation) was found after the 3D printed prototype was finished.

(c) The developed FBG hoop-strain sensor can be used to measure both deformation change and average contact pressure with mounted cylinders. Calibration tests indicate that the new FBG hoop-strain sensor can be used to measure circumferential strain change with a related measurement sensitivity and minimum resolution of 4.04 nm/% and 2.475 $\mu\varepsilon$, respectively.

(d) Monitoring test of a PE cylinder in uniaxial test indicates that the FBG hoop-strain sensor can also be used to measure the vertical pressure of the PE cylinder with a measurement sensitivity and minimum resolution of 0.0035 nm/kPa, and 0.286 kPa, respectively. Measurement range of the hoop-strain sensor is larger than 0-800 kPa in uniaxial compression test with a measurement error less than 7.1%.

Some other filaments such as ABS, PVA, and carbon fiber may replace PLA filament to fabricate sensor components with different mechanical properties. Carbon fiber is a good candidate material to fabricate the sensor components with better stability and durability in comparison with PLA filament. Further studies will carry out focusing on the

development of FBG sensor with carbon fibers and the investigation of material property change such as temperature and deformation change during and after printing process. In addition, only one sample was prepared and tested, multiple sensors will be fabricated and calibrated in future to verify the repeatability of the proposed manufacturing process and their measurement performance.

REFERENCES

[1] C. Hong, Y. Zhang, Y. Yang, and Y. Yuan, "A FBG based displacement transducer for small soil deformation measurement," *Sens. Actuators A, Phys.*, vol. 286, pp. 35–42, Feb. 2018.

[2] C.-Y. Hong, Y.-F. Zhang, and L.-Q. Liu, "Application of distributed optical fiber sensor for monitoring the mechanical performance of a driven pile," *Measurement*, vol. 88, pp. 186–193, Jun. 2016.

[3] Z.-G. Jia, L. Ren, H.-N. Li, S.-C. Ho, and G.-B. Song, "Experimental study of pipeline leak detection based on hoop strain measurement," *Struct. Control Health Monitor.*, vol. 22, no. 5, pp. 799–812, May 2015.

[4] L. Ren, T. Jiang, Z.-G. Jia, D.-S. Li, C.-L. Yuan, and H.-N. Li, "Pipeline corrosion and leakage monitoring based on the distributed optical fiber sensing technology," *Measurement*, vol. 122, pp. 57–65, Jul. 2018.

[5] J. Mao, J. Chen, L. Cui, W. Jin, C. Xu, and Y. He, " Monitoring the corrosion process of reinforced concrete using BOTDA and FBG sensors," *Sensors*, vol. 15, no. 4, pp. 8866–8883, Apr. 2015.

[6] L. Zou, O. Sezerman, and W. Revie, "Pipeline corrosion monitoring by fiber optic distri butedstrain and temperature sensors," in *Proc. NACE Int. Corrosion Conf. Expo*, New Orleans, LA, USA, Mar. 2008, pp. 16–20.

[7] L. Ren, Z.-G. Jia, H.-N. Li, and G. Song, "Design and experimental study on FBG hoop-strain sensor in pipeline monitoring," *Opt. Fiber Technol.*, vol. 20, no. 1, pp. 15–23, Jan. 2014.

[8] T. Jiang, L. Ren, Z. Jia, D. Li, and H. Li, "Application of FBG based sensor in pipeline safety monitoring," *Appl. Sci.*, vol. 7, no. 6, p. 540, May 2017.

[9] L. Ren, T. Jiang, D.-S. Li, P. Zhang, H.-N. Li, and G.-B. Song, "A method of pipeline corrosion detection based on hoop-strain monitoring technology," *Struct. Control Health Monitor.*, vol. 24, no. 6, Jun. 2017, Art. no. e1931.

[10] J.-C. Hao, J.-S. Leng, and Z. Wei, "Non-destructive evaluation of composite pressure vessel by using FBG sensors," *Chin. J. Aeronaut.*, vol. 20, no. 2, pp. 120–123, Apr. 2007.

[11] L. Fang, T. Chen, R. Li, and S. Liu, "Application of embedded fiber Bragg grating (FBG) sensors in monitoring health to 3D printing structures," *IEEE Sensors J.*, vol. 16, no. 17, pp. 6604–6610, Sep. 2016.

[12] K. Willis, E. Brockmeyer, S. Hudson, and I. Poupyrev, "Printed optics: 3D printing of embedded optical elements for interactive devices," in *Proc. 25th Annu. ACM Symp. User Interface Softw. Technol.*, Oct. 2012, pp. 589–598.

[13] T. M. Llewellyn-Jones, B. W. Drinkwater, and R. S. Trask, "3D printed components with ultrasonically arranged microscale structure," *Smart Mater. Struct.*, vol. 25, no. 2, Jan. 2016, Art. no. p. 02LT01.

[14] M. G. Zubel, K. Sugden, D. Sáez-Rodríguez, K. Nielsen, and O. Bang, "3D printed sensing patches with embedded polymer optical Fibre Bragg gratings," *Proc. SPIE*, vol. 9916, May 2016, Art. no. 99162E.

[15] H. Yang, W. R. Leow, and X. Chen, "3D printing of flexible electronic devices," *Small Methods*, vol. 2, no. 1, Jan. 2018, Art. no. 1700259.

[16] C. Hong, Y. Zhang, Z. Lu, and Z. Yin, "A FBG tilt sensor fabricated using 3D printing technique for monitoring ground movement," *IEEE Sensors J.*, vol. 19, no. 15, pp. 6392–6399, Aug. 2019.

[17] L. Wang, T. Meydan, and P. Williams, "Design and evaluation of a 3-D printed optical sensor for monitoring finger flexion," *IEEE Sensors J.*, vol. 17, no. 6, pp. 1937–1944, Mar. 2017.

[18] C. Hong, Y. Zhang, and L. Borana, "Design, fabrication and testing of a 3D printed FBG pressure sensor," *IEEE Access*, vol. 7, pp. 38577–38583, 2019.

[19] S. Umesh, S. Padma, T. Srinivas, and S. Asokan, "Fiber Bragg grating goniometer for joint angle measurement," *IEEE Sensors J.*, vol. 18, no. 1, pp. 216–222, Jan. 2018.

[20] P. Liacouras, G. Grant, K. Choudhry, G. Strouse, and Z. Ahmed, "Fiber Bragg gratings embedded in 3D-printed scaffolds," Aug. 2015, *arXiv:1508.01156*. [Online]. Available: https://arxiv.org/abs/1508.01156

[21] Y.-K. Lin, T.-S. Hsieh, L. Tsai, S.-H. Wang, and C.-C. Chiang, "Using three-dimensional printing technology to produce a novel optical fiber Bragg grating pressure sensor," *Sensors Mater*, vol. 28, no. 5, pp. 389–394, Jun. 2016.

[22] M. G. Zubel, K. Sugden, D. J. Webb, D. Sáez-Rodríguez, K. Nielsen, and O. Bang, "Embedding silica and polymer fibre Bragg gratings (FBG) in plastic 3D-printed sensing patches," *Proc. SPIE*, vol. 9886, Apr. 2016, Art. no. 98860N.

[23] A. Kantaros and D. Karalekas, "Fiber Bragg grating based investigation of residual strains in ABS parts fabricated by fused deposition modeling process," *Mater. Des.*, vol. 50, pp. 44–50, Sep. 2013.

CHENGYU HONG was born in Haerbin, Heilongjiang, China, in 1982. He received the Ph.D. degree in geotechnical engineering from The Hong Kong Polytechnic University, Hong Kong, China, in 2011. His research areas were related to the field of application of different optical fiber sensor technologies in geotechnical engineering. He has developed a number of different optical fiber sensor-based sensors, which have been successfully applied in various research fields during Ph.D. studies. He is currently an Associate Professor with the College of Civil and Transportation Engineering, Shenzhen University, focusing on the development of new functional sensors using different sensing technologies. He is currently a reviewer for more than 30 SCI journals and conference proceedings.

YIFAN ZHANG was born in Luoyang, Henan, China, in 1983. She received the Ph.D. degree from the Institute of Textiles and Clothing, The Hong Kong Polytechnic University, Hong Kong, China, in 2013. After graduation, she joined the Knitting and Clothing Department, College of Textiles, Donghua University, Shanghai, China. Her research interests include development of smart sensors for textile monitoring and digital textile engineering.
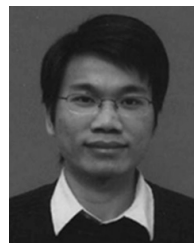
DONG SU received the Ph.D. degree in geotechnical engineering from The Hong Kong University of Science and Technology, in 2005. He is currently a Professor with the College of Civil and Transportation Engineering, Shenzhen University. His research interests include interaction between soil and piles, soil structures fabrication and analysis using 3D printing method, microstructure analysis of soils, and intelligent infrastructures.

ZHENYU YIN is currently an Associate Professor with the Department of Civil and Environmental Engineering, The Hong Kong Polytechnic University. He has 15 years of experiences in, micromechanics, constitutive modeling, multi-scale and multi-physics modeling, optimization methods, since 2003. He has published 101 papers in SCI journals, 31 technical papers in other journals, and four books in his research areas.

• • •